

Seawater Flow Control: Wall Normal ElectroMagnetic Actuators

ROSSI Lionel and THIBAUT Jean-Paul

LEGI, BP 53, 38041 GRENOBLE, France

lionel.rossi@hmg.inpg.fr

jean-paul.thibault@hmg.inpg.fr

<http://www.legi.hmg.inpg.fr>

ABSTRACT

This work deals with ElectroMagnetic Flow Control. Basic mechanisms involved, by the use of wall normal EM actuator, for turbulence intensity and skin friction reduction or coherent structure extinction are approached.

First, EM actuator and its modes of action are described. This description included: some generality on EM actuator; the pack of equation suitable to EM control in seawater; Dimensionless parameters associated with EM control in seawater; EM actuators modes of action.

Second, some experimental investigations have been realised on: Near wall vortex around the actuator; suction zone above the actuator; wall jets around the actuator; seawater tunnel boundary layers visualisation.

INTRODUCTION

ElectroMagnetic (EM) Flow Control deals with the concept of using in combination “wall-flush” electrodes (\mathbf{j} , DC current supply) and “sub-surface” magnets (\mathbf{B} , magnetic induction origin) to create directly local body forces ($\mathbf{j} \times \mathbf{B}$) within a seawater boundary layer. These $\mathbf{j} \times \mathbf{B}$ forces can act directly on velocity and vorticity components, close to the wall.

The electromagnetic Forces distribution can be managed either for drag reduction or local prevention of specific events like flow separation or structure production.

At least two different approaches are possible for flow control by the means of Lorentz forces. First, local schemes are meant to detect and suppress a turbulent event by injecting body forces as it passes over an actuator, see [1, 2, 3, 4]. Second, global schemes are meant to break self-sustaining wall turbulence by imposing new velocity and vorticity components in the wall region.

In this work a group of two permanent magnet poles and two electrodes will be called EM actuator, see Figure 1a&d. Firstly, a brief description of EM actuators is made with a presentation of analytical results used to identify driving terms and modes of action on boundary layer. Secondly experimental results showing some mechanisms of EM control are presented. In these experiments the EM

actuator is placed either in an aquarium (initially at rest) or in a seawater tunnel with a boundary layer eventually including hairpin structures generated by a wall hemisphere, Acalar & Smith [5].

In order to present a step-by-step comprehensive model of some physical mechanisms involved in electromagnetic flow control the present work is based on analytical models. This modelling is progressively upgraded to give an actual description of a very complex reality and finally to get a more predictive scheme.

EM ACTUATOR AND ITS MODES OF ACTION

1. Generality

Nosenchuck & Brown 1993 [6] have shown significant turbulent intensity reduction and drag reduction using a network of wall normal EM actuator; see Figure 1b. Henoeh & Stace 1995 [7] and Weier et al 2000 [8] have shown a flow separation prevention using electrodes and magnets both parallel to the mean flow direction, producing Lorentz forces parallel to the wall.

Figure 1a schematics a typical wall normal EM actuator. The magnetic field is generated by the permanent magnets N and S while the positive and negative electrodes are placed between and perpendicular to the magnets. The distances between respectively magnets and electrodes are quite the same. All components are flush to the wall and significant vorticity sources occurred directly above the magnets. Forces are wall normal above the centre of actuator and are 3D centripetal all around and above, see Figure 2.

EM forces can pump fluid in the wall region leading to new velocity components as well as vorticity sources, within the boundary layer. In fact the general equations are affected by EM forces, which add new terms as well in Navier Stokes equation as in vorticity equation.

2. Equation suitable to EM control in seawater

The governing fluid's equations are (1) the continuity, (2) the Navier Stokes equation with the extra electromagnetic term due to Lorentz forces, (3) the vorticity equation that is the curl of (2). They are written

in the Table 1, with magnetic and electric equations. The magnetic induction \mathbf{B} equation reduces to a Laplace equation (4) due to the very poor conductivity of seawater. In the Ohm's law (5), describing the current density \mathbf{j} , $\mathbf{u} \times \mathbf{B}$ is negligible compared to \mathbf{E} the imposed electric field.

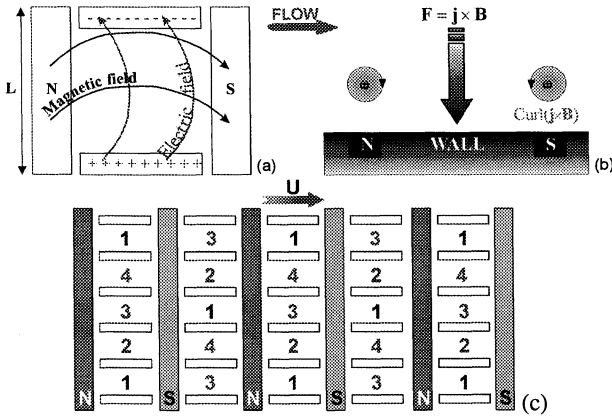


Figure 1: Wall normal actuator: **a)** Front view of magnets and electrodes arrangement at the wall. **b)** Cross section view of magnets in wall. Sources of EM vorticies in the boundary layer due to Lorentz forces are indicated by ω . **c)** Actuators network, up view illustration of 4 first phases of power supply on a same board. **d)** EM actuator 1999

Fluid's equations	
$\text{div } \mathbf{u} = 0$	(1)
$\rho \frac{d\mathbf{U}}{dt} + \nabla P + \rho \mathbf{g} = \mu \nabla^2 \mathbf{U} + \mathbf{j} \times \mathbf{B}$	(2)
$\rho \frac{d\omega}{dt} = \rho \omega \cdot \nabla \mathbf{U} + \mu \nabla^2 \omega + \nabla \times (\mathbf{j} \times \mathbf{B})$	(3)
Magnetic induction equation and Ohm's law	
$\frac{\partial \mathbf{B}}{\partial t} = \text{curl}(\mathbf{u} \times \mathbf{B}) + \frac{1}{\mu \sigma} \nabla^2 \mathbf{B} \Rightarrow \nabla^2 \mathbf{B} \approx 0$	(4)
$\mathbf{j} = \sigma (\mathbf{E} + \mathbf{u} \times \mathbf{B})$	(5)
$\text{div } \mathbf{B} = 0$ and $\text{div } \mathbf{j} = 0$	(6)

Table 1: Fluid, magnetic and electric equations used in seawater EM control

3. Dimensionless parameters associated with EM control in seawater

It is worthwhile to identify possible mechanisms of EM control in seawater and to this end, dimensional analysis is useful. The typical parameters chosen are: (i) Actuator Length $L_{EM} \sim 10^{-2}$ m, (ii) magnetic induction $B \sim 1$ T, (iii) Imposed electric field $E \sim 10^3$ V/m, (iv) Electrical conductivity of seawater $\sigma \sim 5$ S/m, (v) Seawater magnetic permeability $\mu = 4\pi \cdot 10^{-7}$ H/m, (vi) Flow velocity $U \sim 1$ to 10 m/s, and (vii) Boundary layer thickness $\delta \sim 10^{-3}$ to 10^{-2} m. The Reynolds number R_{ex} is

in order of 10^6 or more. Table 2 is constructed with the hypothesis of an action zone of forces taller than the boundary layer thickness, see [9].

Viscous parameter	
$\frac{\text{EM term}}{\text{Viscous term}}$	$H_a^2 = \frac{\sigma E B \delta^2}{\rho \nu U} \approx 1$ (7)
Inertial parameters I : (Interaction parameters)	
Effect on longitudinal component	$I_U = \frac{\sigma E B}{\rho U^2} = \frac{\sigma E B \delta}{\rho U^2} \approx 10^{-4}$ to 10^{-2} (8)
Effect on normal component	$I_V = \frac{\sigma E B}{\rho V^2} = \frac{\sigma E B \delta}{\rho V^2} \approx 10$ to 10^4 (9)
Effect on a local velocity fluctuation	$I_{vloc} = \frac{\sigma E B}{\rho v^2 l} \approx 10^{-4}$ to 10^{-1} (10)

Table 2: non dimensional parameters associated with EM flow control

The Hartmann number, cf. (7), is of order of one. So, in the boundary layer, EM forces injected in the flow are comparable with viscous terms. Various interactions parameters are evaluated which compare EM forces with inertial terms associated to different velocity scales: (8), (9), (10). The strongest parameter appears on the mean wall normal component (9). Thus the normal mean flow is expected to be dominated by the EM forces even though the longitudinal external flow will be non-affected (8). The moderate local interaction parameter based on a local velocity fluctuation (10) demonstrates that EM actuator must be adapted in size and power to kill "a turbulent event".

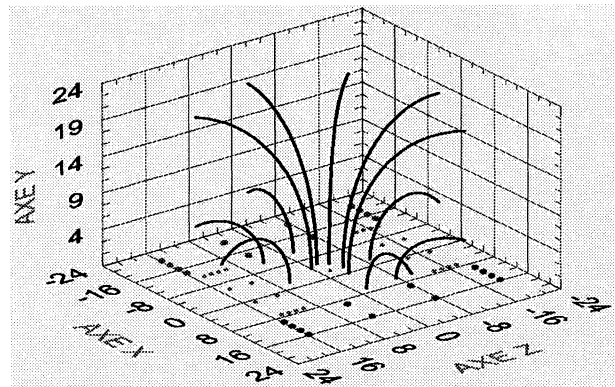


Figure 2: 3D view of computed EM forces lines above an actuator placed in the bottom plan of the schematic.

4. EM actuators modes of action:

After this brief description of general equations and dimensionless parameters terms, the following global descriptive remarks are useful for a better understanding of EM actuators modes of action:

① The electromagnetic fields as well as the induced forces developed above an EM actuator are 3D. A typical shape of forces lines ($\mathbf{f} \times \mathbf{dl} = 0$) obtained by analytical computations is showed in figure 2. EM forces above the actuator have a quasi-concentric distribution and are

distributed like a siphon shape. The direction of forces is mainly normal to the wall and their sign directly depends on current's sign (i.e. up or down).

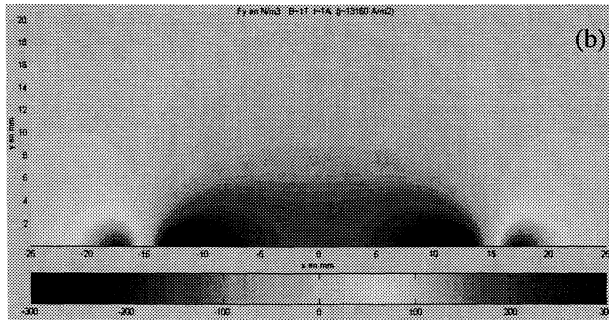
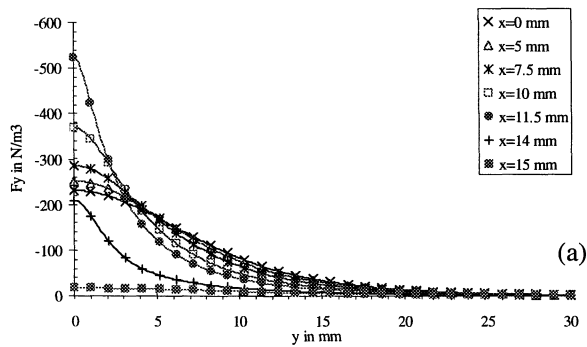


Figure 3: Computed wall normal component F_y in N/m^3 of EM forces in a plan normal to wall and magnet, at the centre line of EM actuator ($z=0$), Actuator 1999, (a): $B=1T$, $I=1.1A$, $J=14\ 500A/m^2$; (b): $B=1T$, $I=1A$, $J=13\ 160A/m^2$.

② The magnetic and electric field both decrease from the wall ($y=0$) towards the external flow. Therefore the magnitude of the forces is maximum at the wall. Numerical results on wall normal component of $\mathbf{j} \times \mathbf{B}$, see (2) forces are showed on Figure 3. For a 1A current and $B \sim 1T$, f_y intensity is of order of $-100\ N/m^3$, in a zone having the actuator width, $L=30\ mm$ (see Figure 1), and with a height near of $L/5$.

③ $\mathbf{j} \times \mathbf{B}$ forces are rotational, they induce vorticity components which are distributed all around the EM actuator, see figure 4 (c). An experimental demonstration of this is obtained by dye injection and visualisation of large coherent structures. Figure 4a&b shows such a structure after a 5 seconds actuation starting from flow initially at rest. The typical length scale of the structure is ten times larger than the actuator length (L). Rotation's tubes parallel to magnet or electrodes and mushroom shape in the angles can be noticed.

EXPERIMENTAL INVESTIGATION OF WALL NORMAL ACTUATORS

The experiments reported are obtained either in an aquarium ($50 \times 60 \times 50$) or in seawater test loop. The maximum flow rate is $60\ m^3/h$. The small visualisation tunnel $4\ cm \times 4\ cm \times 100\ cm$ correspond to a maximum velocity of $10.4\ m/s$ but a strong confinement. The large visualisation tunnel $10\ cm \times 10\ cm \times 130\ cm$ correspond to a

maximum velocity of $1.66\ m/s$ with a moderate confinement.

Two wall normal actuator are used: i) Actuator 1999 with a magnet shape of $8\ mm$ height, $35\ mm$ length and $5\ mm$ wide. ii) Actuator 2000 with a magnet of $20\ mm$ height, $45\ mm$ length and $5\ mm$ wide. For each actuator B induction is $0.65T$ at surface pole, electrode surface is $4\ mm \times 19\ mm$.

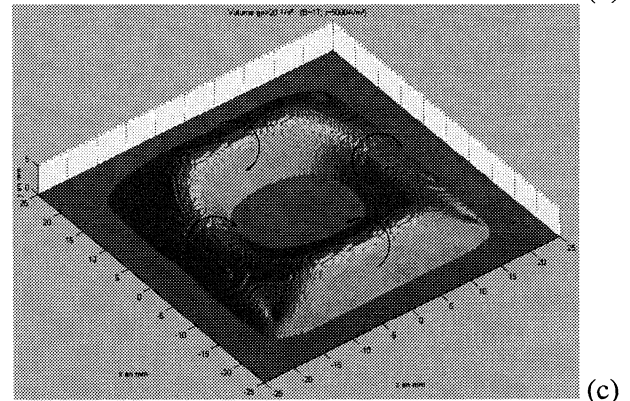
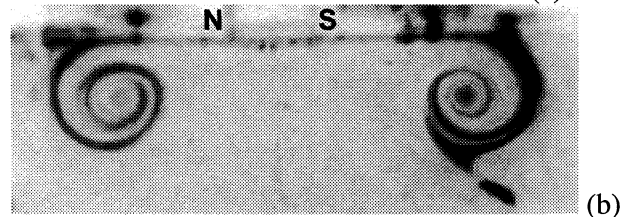
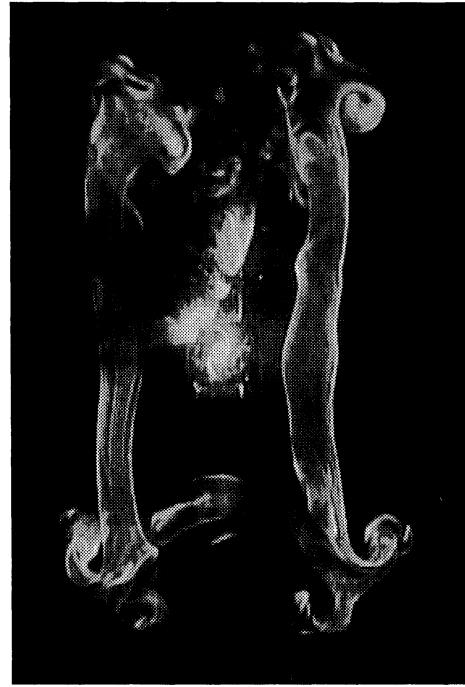


Figure 4: (a)&(b): Saltwater ($35g\ NaCl/l$) aquarium visualisation: (a) front view of vortical structure developing above the EM actuator in a flow initially at rest ($I=1.1A$, time ~ 5 seconds, $B \sim 0.65T$); (b) cut view of vortical structure developing above the EM actuator. (c) Computed 3D zone where EM forces rotation source is larger than $20\ rad/s^2$ (given by $F/\rho * \text{Curl } \mathbf{f}$; with $\mathbf{F}=\mathbf{Ff}$); $B \sim 1T$, $I=1.1A$, $J=14\ 500\ A/m^2$, $L=30\ mm$. (Actuator 1999)

1. Near wall vortex around the actuator:

PIV measurements, see Figure 5, are realized in the central wall normal plan ($z=0$) of the actuator just at the edge of the actuator $x=13$ to 37 mm. The flow is initially at rest in a transparent test section of $10\text{cm}\times 10\text{cm}\times 130\text{cm}$. The measurements confirm visualisation by fluoresceine (Figure 4a&b) and the presence of vorticity in the flow due to EM action. Both type shear (or local rotation) and flow's rotation can be observed on Figure 5a, which combine vorticity's scalar (colour scale) and velocity's arrows. Near the wall, the wall jet imposes a shear type vorticity with alternative negative and positive signs. At some distance from the wall ($y=5.25$ mm and $x=30.86$ mm) a vortex core is clearly apparent. The triangular shapes of vorticity profiles (see Figure 5b&c) clearly show that the apparent structure is a complex vortex and not only a solid rotation one. This PIV result completes visualisations of vortical structures injected in aquarium initially at rest, when the power is put ON, see [9].

2. Suction zone above the actuator

PTV measurements, see Figure 6c, are realised in the central wall normal plan ($z=0$) above the centre of the actuator. A large scale view of the flow $y=8$ mm to 50 mm shows that the so-called "suction zone" EM forces pumped fluid, is much larger than attraction zone of EM forces, see Figure 6a&b.

The Figure 6c gives a view of intensity and distribution of suction velocity compared with solid lines for computed EM forces. Maximum suction velocity is about 14 mm/s and is essentially normal to the wall. The suction zone is equivalent to the actuator size L , as well for its width as for its height. This suction zone is larger than the zone where EM forces are strongly present, which height is only $L/5$. Of course due to increasing forces near the wall and to the work of body forces along a flow's current line, the suction velocity increases as distance normal to the wall decreases.

A simplified computation, considering the work of forces as a prime mover, seems to be a good approximation to evaluate velocity variation versus currents intensity. The measured normal velocity evolution with y (on the axis of EM actuator) is plotted for different currents intensity on figure 7. The computed velocities are over plotted in solid lines. It demonstrates the very good agreement between predictions and measurements, which confirm that the EM pumping is mostly balancing the inertia of the flow.

3. Wall jets around the actuator

Both flow conservation and presence of the wall, drives the EM pumped flow to create wall jets all around the actuator.

PTV measurements are also repeated in the corners of the actuator, in a plan wall normal and passing at the corner between magnets and electrodes ($\sim 45^\circ$), see Figure 9. The velocity of wall jets is larger than the typical velocity in the suction zone. It appears that these wall jets are related to the development of the coherent structure showed in figure 5. Wall jets are brutally sucked and

disappear meanwhile passing under coherent vortical structures. In the present experiments the jet velocity at the actuator's corners is larger than in other region and the thickness of the jet is smaller. These corners region of EM actuator corresponds to region with a lack of forces opposed to the local flow. The maximum velocity of the jet at actuator's corners is about 50 mm/s. Thickness of these corner's jet is about $L/10$ i.e. 3 mm. are given in Figure 8.

4. Seawater tunnel boundary layers visualisation

To analyse the effects of EM forces in a boundary layer, numerous visualisations are performed in a seawater tunnel having a transparent test section $4\text{cm}\times 4\text{cm}\times 1\text{m}$. Pumping of EM forces is able to attract or repulse, depending on forces sign, either a laminar boundary layer or a boundary layer including hairpin structures generated by a wall hemisphere [7]. Effect of EM actuator on a hairpin street is given in Figure 8. The competition between the effects of flow normal to the wall induced by Lorentz forces and hairpin structure may be one of the keys controlling the time and capability of killing structure by a single shot or multiple (network) shot. It has been observed that with an attracting effect, structures tend to disappear much faster than without EM action. They degenerate very quickly down flow the actuator.

CONCLUSION

EM actuator is a mean to directly apply local 3D Lorentz forces in the flow. These local body forces are associated with additional terms in Navier Stokes equation as well as in vorticity equation. EM forces are able to pump or to deflect flow near the wall as well as to inject vorticity sources. So each component of velocity or vorticity is altered by electromagnetic control either directly during actuation or after due to a persisting induced velocity (normal component and wall jets) or vorticity.

In regions of the boundary layer where normal velocity is weak, EM actuators impose a new component of normal velocity. In zone where turbulent events introduce wall normal velocity, EM control can counteract on and around these events. So EM control may be able as well to change the "wall information" of the flow and so to break the turbulence regeneration cycle as to alter turbulence by "killing events" as soon as detected.

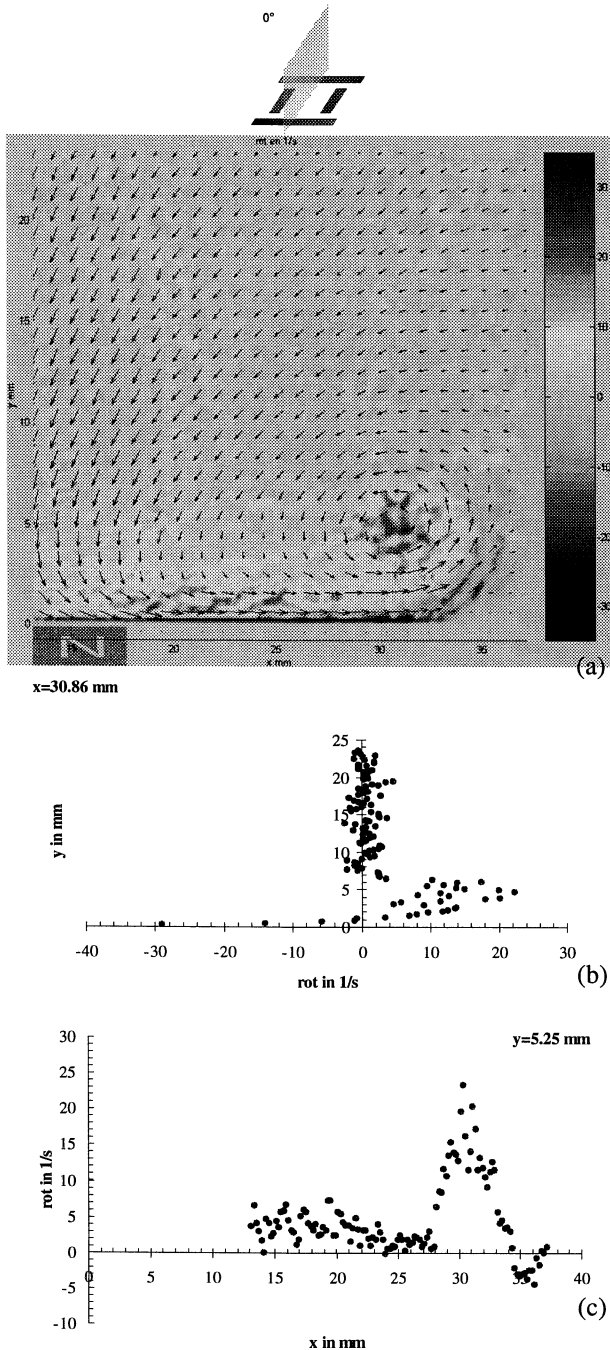


Figure 5: PIV measurement of vorticity after 3 s of actuation, without forced flow, $I=1.73$ A. Transparent test section of $10\text{ cm} \times 10\text{ cm} \times 130\text{ cm}$. (a): scalar map of vorticity, arrows represent flow velocity, only one arrow for five measurements points is plotted. (b) & (c): profiles of vorticity in vertical and horizontal medians plan of apparent vortex in left scalar map. (Actuator 2000)

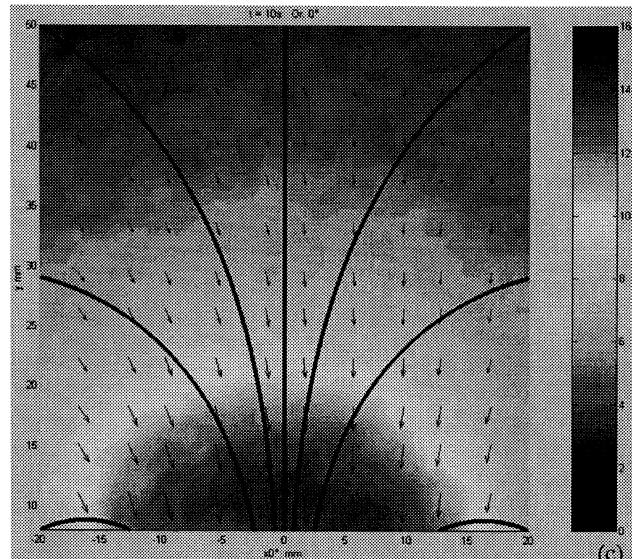
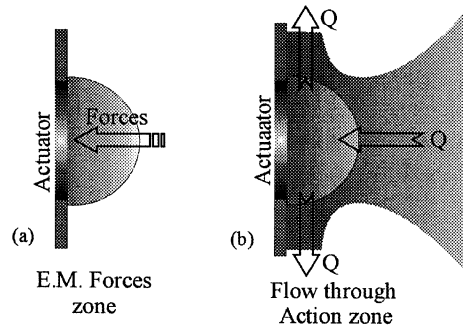


Figure 6: (a) & (b): schematic representation of action zone: forces and pumped flow. (c): PTV of suction velocity (colour in mm/s and arrows) and computed EM forces solid lines in a plan normal to wall and magnet, at the centre line of EM actuator ($z=0$); $B \sim 0.65\text{ T}$ at magnets surface, $J=14\ 500\ \text{A/m}^2$, $I=1.1\text{ A}$, $L=30\text{ mm}$, 10 s actuation. (Actuator 1999)

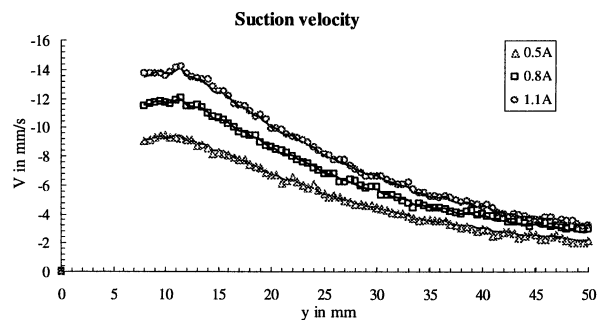


Figure 7: PTV analysis of wall normal suction velocity on actuator's axis ($x = z = 0$). Δ plot corresponds to $I=0.5\text{ A}$ i.e. $6\ 600\ \text{A/m}^2$; \square plot corresponds to $I=0.8\text{ A}$ i.e. $10\ 500\ \text{A/m}^2$; \circ plot corresponds to $I=1.1\text{ A}$ i.e. $14\ 500\ \text{A/m}^2$. Solid lines over plotted represent similitude prediction (based on forces action) of velocity variation due to currents. (Actuator 1999)

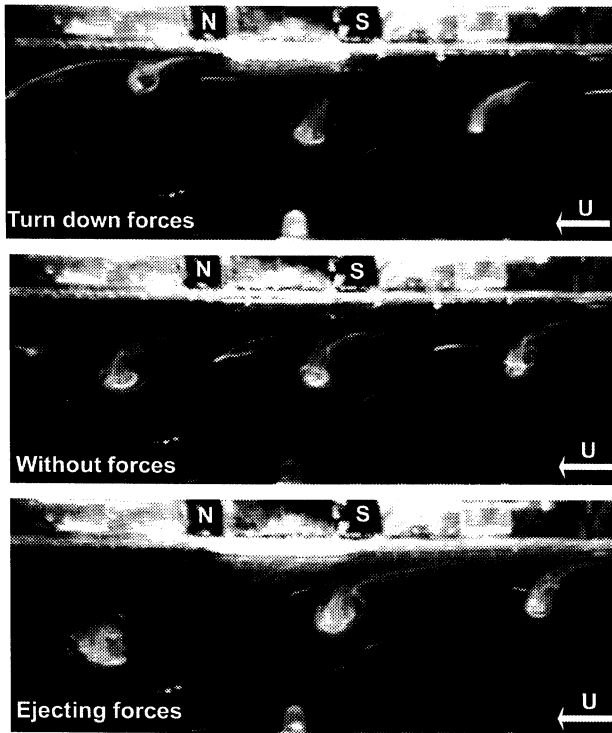


Figure 8: Seawater (35g NaCl/l) tunnel visualisation: EM forces action on hairpin structures ($U_{\infty} \approx 0.1$ m/s, $I \approx 1.1$ A, $B \sim 0.65$ T at magnet's pole). Flow is directed from right to left.

ACKNOWLEDGMENTS

DGA/BEC and DGA/DSP ; "service repro-visu" of ENSHMG and his director Mr. F. Bonnel; Dr O. Cugat and Dr J. Delamare of LEG-ENSIEG ; Dr. Franck Mc Cluskey ; Dr S. Tardu ; P. Carrechio and M. Kusulga of LEGI.

REFERENCES

- [1] ROBINSON; 1991, « Coherent motions in the turbulent boundary layer », *Annu. Rev. Fluid. Mech.* 23 :601-39.
- [2] ADRIAN, MEINHART, TOMKINS; 2000, « Vortex organization in the outer region of the turbulent boundary layer », *J. Fluid Mech.* Vol 422, pp1-54.
- [3] SMITH; 1998, « Vortex developpement and interactions in turbulent boundary layers : implications for surface drag reduction », *Proc. of the Int. Symp. on Seawater Drag Reduction, Newport R. I.*, pp 39-45.
- [4] MENG; 1998; « Engineering insight of near wall microturbulence for drag reduction and derivation of a design map for seawater electromagnetic flow control » *Proc. of the Int. Symp. on Seawater Drag Reduction, Newport R. I.*, pp 359-369.
- [5] ACALAR, SMITH; 1987, « A study of hairpin vortices in a laminar boundary layer part1: hairpin vortices generated by a hemisphere protuberance », *JFM* (1987) vol 175 pp1-41.
- [6] NOSENCHUCK, BROWN; 1993, « The direct control of wall shear stress in a turbulent boundary layer », *Proc. of the Int. Conf. on Near Wall Turbulent Flows, Elsevier* pp 689-698.
- [7] HENOCH, STACE; 1995, "Experimental Investigation of a Salt Water Turbulent Boundary Layer Modified by an Applied Streamwise Magnetohydrodynamic Body Force", *Phys. Fluids* 7,(6) , pp. 1371-1383, June 1995.
- [8] WEIER, FEY, GERBETH, MUTSCHKE, AVILOV; 2000, « Boundary layer control by means of electromagnetic forces » *ERCOFTAC bulletin N°44*, mars 2000 pp37-41.
- [9] THIBAUT, ROSSI; 2000, « Experimental modeling of seawater electromagnetic flow control », *ERCOFTAC bulletin N°44*, mars 2000 pp 41-49.

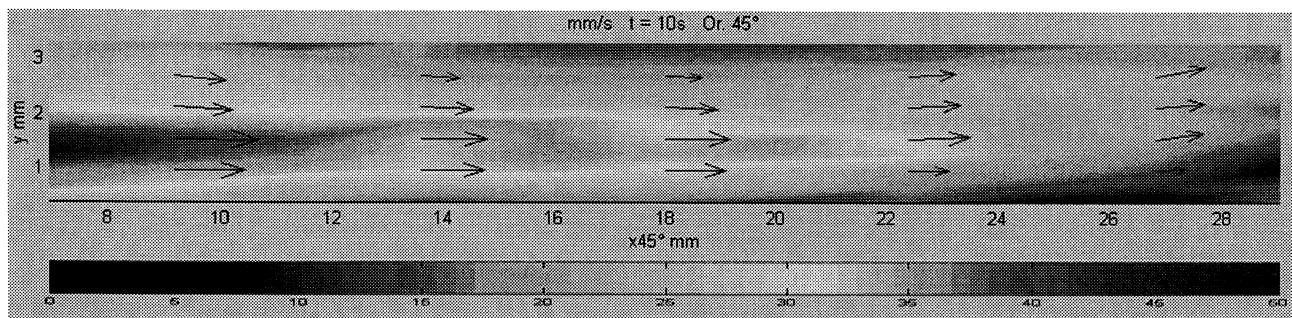


Figure 9:PTV of jet velocity at EM actuator's corner, $B \sim 0.65$ T at magnets surface, $I = 1.1$ A, $J = 14\ 500$ A/m² at electrodes surface, 10 s actuation. $x_{45^\circ} = 0$ at actuator's corner. (Actuator 1999)